Intramolecular Triplet Energy Transfer via Higher Triplet Excited State during Stepwise Two-Color Two-Laser Irradiation

Yosuke Oseki, Mamoru Fujitsuka, Masanori Sakamoto, and Tetsuro Majima*

The Institute of Scientific and Industrial Research (SANKEN), Osaka University, Mihogaoka 8-1, Ibaraki, Osaka 567-0047, Japan

Received: May 25, 2007; In Final Form: July 12, 2007

We studied the energy transfer processes in the molecular array consisting of pyrene (Py), biphenyl (Ph_2), and bisphthalimidethiophene (ImT), $(Py\text{-}Ph_2)_2$-ImT, during two-color two-laser flash photolysis (2-LFP). The first laser irradiation predominantly generates ImT in the lowest triplet excited state ($ImT(T_1)$) because of the efficient singlet energy transfer from Py in the lowest singlet excited state to ImT and, then, intersystem crossing of ImT. $ImT(T_1)$ was excited to the higher triplet excited state (T_n) with the second laser irradiation. Then, the triplet energy was rapidly transferred to Py via a two-step triplet energy transfer (TET) process through Ph_2. The efficient generation of $Py(T_1)$ was suggested from the nanosecond−picosecond 2-LFP. The back-TET from $Py(T_1)$ to ImT was observed for several tens of microseconds after the second laser irradiation. The estimated intramolecular TET rate from $Py(T_1)$ to ImT was as slow as 3.1×10^4 s^{-1}. Hence, long-lived $Py(T_1)$ was selectively and efficiently produced during the 2-LFP.

Introduction

Energy transfer in molecular arrays is one of the fundamental processes in photochemistry. Successive fast singlet energy transfer (SET) processes across long distance play an important role in harvesting the photon energies to the photosynthetic reaction center.[1] To fabricate artificial light conversion systems, intramolecular energy and electron-transfer processes have been extensively investigated for various molecular assemblies.[2]

Controlling the intramolecular energy and electron-transfer reactions using multistep photoirradiation is particularly important to achieve all photodriven molecular logic devices.[3] The higher triplet excited state (T_n, $n \geq 2$) will be one of the important intermediates in molecular devices. Because the T_n states are generated by the two-step photoirradiation they often induce photoionization, energy and electron transfer, and bond dissociation, even when these processes are energetically impossible from the lowest singlet (S_1) and triplet (T_1) excited states.[4,5] Only a few papers have reported the intramolecular triplet energy transfer (TET) from the T_n state.[6] McGimpsey et al. proposed a molecular scale shift register using the intramolecular TET from phenanthrene(T_n) to naphthalene via center biphenyl in the triad system in which chromophores were linked by methyl ester tethers.[6a] However, the efficiency and/or selectivity of the TET seems to be low because the distance between the chromophores is too long to achieve the efficient TET from phenanthrene(T_n) to biphenyl due to the methyl ester tether, and the possibility of back-TET to phenanthrene cannot be ruled out even though biphenyl(T_1) was produced. In addition, C−O bond dissociation from the T_n state has recently been reported for the ester tether.[5b,c,f] Therefore, refined molecular architecture is required to utilize the TET from the T_n state, since the T_n states usually have excessive energy and quite short lifetime.[7]

On the other hand, Hayes et al. revealed the intramolecular TET processes in the dyad molecules of Zn-porphyrin and perylene monoimide, in which Zn−porhyrin was connected at the imide-nitrogen or the 9-position of the perylene core.[6b] Interestingly, the TET rate from Zn−porphyrin(T_1) to perylene monoimide significantly depends on the linking position. The TET rates were estimated to be 55 ns and 7 ps for the dyads with linkage at the imide-nitrogen and the perylene core, respectively, while the TET from perylene(T_n) to Zn−porphyrin was extremely fast (600 fs) in the both dyads. These TET behaviors were explained by the low electron density at the imide-nitrogen, and it was suggested that the electronic configuration of perylene(T_n) is different from that in the T_1 state.

In the present study, we report the energy transfer processes in a linear molecular array consisting of pyrene (Py), biphenyl (Ph_2), and bisphthalimidethiophene (ImT) [$(Py\text{-}Ph_2)_2$-ImT, Figure 1], during two-color two-laser flash photolysis (2-LFP). $(Py\text{-}Ph_2)_2$-ImT was newly designed to achieve the selective, long range, and efficient intramolecular TET by using the 2-LFP. $ImT(T_1)$ generated with the first laser flash is excited to the T_n state during the second laser irradiation. As Hayes et al. have reported, the TET from $ImT(T_n)$ to Ph_2 is expected to occur rapidly. The imide bond decelerates the back-TET from $Ph_2(T_1)$ to ImT, while the TET from $Ph_2(T_1)$ to Py takes place predominantly, since Py and Ph_2 are connected by a methylene spacer.[8] Thus, it is expected that $Py(T_1)$ is selectively and efficiently generated during the 2-LFP, although the lowest triplet energy level (E_{T1}) of Py is higher than that of $ImT(T_1)$. Since the distance between Py and ImT is relatively long, the back-TET from $Py(T_1)$ to ImT occurs slowly (Scheme 1). The present molecular system can improve the efficiency of selective sensitization reactions by 2-LFP, such as energy and electron transfer, when the reaction can occur from $Py(T_1)$, but not from $ImT(T_1)$, and will be a new model of molecular devices driven by multilaser excitation.

Results and Discussion

Molecular Design of $(Py\text{-}Ph_2)_2$-ImT. As Hayes et al. reported, the intramolecular TET from perylene monoimide-

* Corresponding author. E-mail: majima@sanken.osaka-u.ac.jp.

10.1021/jp074062o CCC: $37.00 © 2007 American Chemical Society
Published on Web 09/07/2007

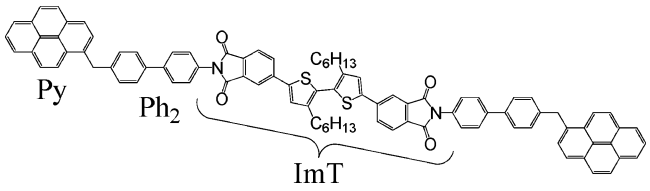

Figure 1. Molecular structure of $(Py\text{-}Ph_2)_2$-ImT.

SCHEME 1: Schematic Energy Diagram of the Intramolecular Triplet Energy Transfer Processes in $(Py\text{-}Ph_2)_2$-ImT during the Two-Color Two-Laser Flash Photolysis

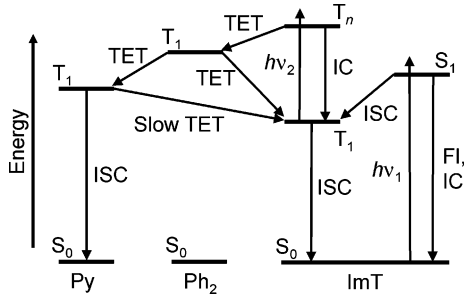

(T_n) to energy acceptor is expected to be extremely fast. However, the perylene mono- and diimide derivatives are known as highly fluorescent molecules.[9] In other words, the quantum yields of intersystem crossing (Φ_{ISC}) are low. On the other hand, naphthalimide derivatives have high Φ_{ISC} values,[10] and have been widely used as a good electron acceptor.[10a,11] High electron-acceptor ability is not favorable in the present study, since the intramolecular charge separation from the singlet excited-state decreases the Φ_{ISC}. In addition, it has been reported that *N*-phenyl substitution of naphthalimides arouses the fast internal conversion.[12] Therefore, we synthesized a new chromophore, i.e., bisphthalimidethiophene (ImT). It is expected that the extended π-conjugation suppresses the fast internal conversion process caused by *N*-phenyl substitution of imide bond, as well as highly fluorescent perylene mono- and diimide derivatives,[9] and the incorporation of bithiophene in the dye molecule decreases the acceptor ability of phthalimide because of the electron-donating ability of oligothiophenes.[13] In addition, oligothiophenes and their derivatives have a large molar absorption coefficient in both the ground and excited states.[14] This property is useful to improve the light-harvesting efficiency.

At first, we synthesized cyclohexyl-substituted ImT [$(CH)_2$-ImT, Figure 2A, inset]. $(CH)_2$-ImT is expected to generate the T_1 and T_n states with the first 355-nm laser and the second 532-nm laser irradiation, respectively (Figures S1, 2). No bleaching of the absorption of $(CH)_2$-ImT(T_1) was confirmed during the nanosecond−nanosecond (ns−ns) 2-LFP (Figure 2A). Therefore, the unimolecular reactions, such as ionization and bond dissociation from ImT(T_n), can be ruled out. On the other hand, the bleaching of the absorption of $(CH)_2$-ImT(T_1) ascribed to the intermolecular TET from $(CH)_2$-ImT(T_n) to 3,3′-dimethylbiphenyl was observed upon the second laser irradiation (Figure 2B), indicating that the energy level of ImT(T_n) is higher than that of 3,3′-dimethylbiphenyl (271 kJ/mol).[5g,15] In addition, the lifetime of $(CH)_2$-ImT(T_1) did not change even in the presence of pyrene molecule at high concentration. Therefore, the energy level of ImT(T_1) is unequivocally lower than that of pyrene(T_1) (E_{T1} = 203 kJ/mol).[15] The energy levels of pyrene(S_1) (E_{S1} = 322 kJ/mol) and biphenyl(S_1) (E_{S1} = 418 kJ/mol) are significantly higher than that of $(CH)_2$-ImT (E_{S1} = 230 kJ/mol) (Figure S1), although the E_{S1} and E_{T1} of Ph_2 are expected to be lower than that of pristine biphenyl, because Ph_2 is connected with the nitrogen atom of the imide bond. The intramolecular energy transfer from Py(S_1) or Ph_2(S_1) to ImT is possible. Therefore, the TET processes in $(Py\text{-}Ph_2)_2$-ImT can be expected to be as shown in Scheme 1.

$(Py\text{-}Ph_2)_2$-ImT was synthesized according to Scheme 2. Details on the synthesis of $(Py\text{-}Ph_2)_2$-ImT are described in Experimental Section.

Steady-State Absorption and Fluorescence Spectra. Figure 3 shows the absorption and fluorescence spectra of $(Py\text{-}Ph_2)_2$-ImT in THF. The sharp absorption peaks at 314, 328, and 345 nm are assigned to Py.[15] On the other hand, the broad absorption band around 380 nm is ImT. The absorption and fluorescence peaks of the ImT moiety were essentially the same as those of $(CH)_2$-ImT (Figure S1), suggesting no or weak interaction between ImT and other chromophores.

The fluorescence from Py moiety appeared at almost the same position as that of pristine pyrene, indicating the negligible interaction between Py and Ph_2, whereas the fluorescence intensity from Py was very weak even when $(Py\text{-}Ph_2)_2$-ImT was excited at 345 nm to excite Py efficiently. The Φ_{fl} of ImT was estimated to be 0.08 (excitation at 400 nm, using sexithiophene as a reference).[14a] Significantly small fluorescence from Py compared to ImT indicates that the Φ_{fl} of Py in the molecular array is $<10^{-2}$, in spite of the large fluorescence quantum yield of pyrene (0.72).[15] In addition, the fluorescence lifetimes of Py moiety of $(Py\text{-}Ph_2)_2$-ImT and 1-methylpyrene were estimated to be 197 ps and 17.0 ns, respectively, suggesting the efficient intramolecular SET from Py(S_1) to ImT. The rate and efficiency of the intramolecular SET were estimated to be 5.0×10^9 s^{-1} and 99%, respectively. Since Ph_2 is also expected to donate the singlet energy to ImT, excitation of $(Py\text{-}Ph_2)_2$-ImT predominantly generates ImT(S_1), which converts to ImT(T_1), independent of the excitation wavelength.

Intramolecular TET in $(Py\text{-}Ph_2)_2$-ImT during Nanosecond−Nanosecond Two-Color Two-Laser Flash Photolysis. The transient absorption spectrum with a peak at 650 nm was observed upon the first 355-nm laser irradiation of $(Py\text{-}Ph_2)_2$-ImT (Figure 4A). This absorption band was assigned to ImT(T_1), since $(CH)_2$-ImT showed the similar T_1 state absorption upon excitation. Although the excitation of $(Py\text{-}Ph_2)_2$-ImT with the 355-nm laser flash generates both Py(S_1) and ImT(S_1), ImT(T_1) is predominantly produced due to the fast SET from Py(S_1) to ImT as described in the former section. The bleaching of the absorption band of ImT(T_1) was observed upon the second 532-nm laser irradiation, while the transient absorption was increased around 415 nm. From the difference spectrum of the transient absorption spectra of $(Py\text{-}Ph_2)_2$-ImT during the 355-nm single-laser flash photolysis and 2-LFP, the generation of the very sharp absorption band with a peak at 415 nm was confirmed (Figure 4B). The absorption band at 415 nm can be assigned to Py(T_1) [pyrene-(T_1): 412.5 nm, ϵ = 30 400 M^{-1} cm^{-1}].[15]

Figure 5 shows the time profiles of ΔOD at 650 and 415 nm during the ns−ns 2-LFP of $(Py\text{-}Ph_2)_2$-ImT in THF. The bleaching of the absorption at 650 nm was observed during the second laser irradiation and it recovered for several tens of microseconds (Figure 5A). At 415 nm, the negative absorption upon the first laser irradiation is attributed to the bleaching of the ground-state absorption of ImT (Figure 5B). The absorption at 415 nm was increased with the second laser irradiation and this change was more apparent compared with the decrease of ΔOD at 650 nm, indicating that the increased absorption at 415 nm is mainly the generation of Py(T_1) and the small contribution of the recovery of ImT in the ground state.

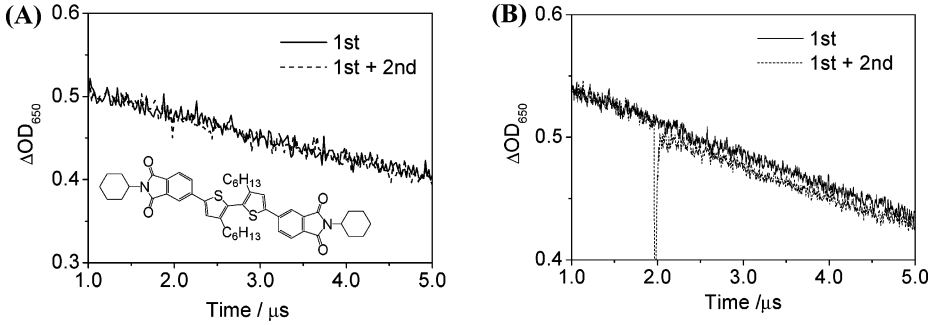

Figure 2. Time profiles of ΔOD at 650 nm of $(CH)_2$-ImT in THF in the absence (A) and presence (B) of 3,3′-dimethylbiphenyl (2.0 M) during the ns−ns 2-LFP (first laser, 355 nm, 5-ns fwhm, 10 mJ pulse^{-1}; second laser, 532 nm, 5-ns fwhm, 20 mJ pulse^{-1}). The second laser was irradiated at 2 μs after the first laser. The solid and dashed lines show the 355-nm single-laser and two-laser flash photolysis, respectively. The spike signal induced by the second laser flash is due to the laser scattering. Inset: molecular structure of $(CH)_2$-ImT.

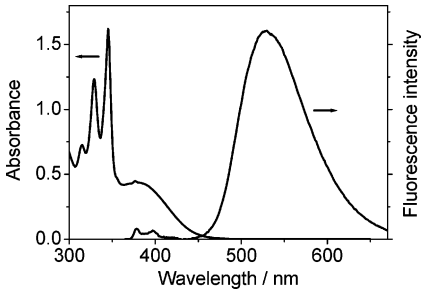

Figure 3. Steady-state absorption and fluorescence spectra of $(Py\text{-}Ph_2)_2$-ImT in THF. The sample was excited at 345 nm to observe the fluorescence spectrum.

The recovery of the absorption change after the second laser irradiation can be assigned to the back-TET from $Py(T_1)$ to ImT. From a single-exponential fit to ΔΔOD between the 355-nm laser flash photolysis and 2-LFP, the recovery rates of $ImT(T_1)$ were estimated to be 15.3 and 15.8 μs at 650 and 415 nm, respectively (Figure 6). These values correspond to the lifetime of $Py(T_1)$. Hence, it was confirmed that relatively long-lived $Py(T_1)$ was generated as a product during the 2-LFP. Both intramolecular and intermolecular TET are considered as the back-TET processes from $Py(T_1)$ to ImT (eqs 1 and 2).

$$(Py(T_1)\text{-}Ph_2)_2\text{-}ImT \xrightarrow{k_{ITET}} (Py\text{-}Ph_2)_2\text{-}ImT(T_1) \quad (1)$$

$$(Py(T_1)\text{-}Ph_2)_2\text{-}ImT + (Py\text{-}Ph_2)_2\text{-}ImT \xrightarrow{k_{ETET}} (Py\text{-}Ph_2)_2\text{-}ImT + (Py\text{-}Ph_2)_2\text{-}Im(T_1) \quad (2)$$

Therefore, the back-TET rate from $Py(T_1)$ to ImT (k_{obs}) is expressed by eq 3.

$$k_{obs} = k_{ITET} + k_{ETET}[(Py\text{-}Ph_2)_2\text{-}ImT] \quad (3)$$

where k_{ITET} and k_{ETET} are the intramolecular and intermolecular TET rate constants from $Py(T_1)$ to ImT, and $[(Py\text{-}Ph_2)_2\text{-}ImT]$ is the concentration of $(Py\text{-}Ph_2)_2$-ImT. From the concentration dependence of k_{bos}, the intramolecular TET rate was estimated to be 3.1×10^4 s^{-1} (Figure 7), equivalent to 32 μs of lifetime.

The relatively large center-to-center distance between Py and ImT ($R = 21.4$ Å) is one of the reasons for the slow back-TET from $Py(T_1)$ to ImT,[8,16] and the broken π-conjugation between Py and ImT by the methylene and imide bonds is also effective to decelerate the back-TET.[17] In addition, the different Py-ImT orientation due to the methylene spacer is considered (Figure S3). A significant effect of donor−acceptor orientation has been observed for the TET in cyclohexane spacer systems.[8] When the benzophenone and naphthalene are connected at 1-equatorial and 4-axial positions, respectively, by a cyclohexane spacer, the intramolecular TET rate is reported to be 30-fold smaller than that of 1,4-equatorial.

The intramolecular TET process from $Py(T_1)$ to ImT slowly occurred. Whereas, the SET from $Py(S_1)$ to ImT was efficient, in other words fast. The difference between the SET and TET comes from the energy transfer mechanism. The TET occurs on the basis of an exchange mechanism.[18] According to the slow back-TET from $Py(T_1)$ to ImT, the exchange coupling between Py and ImT is considered to be small. On the other hand, it is expected that the SET takes place on the basis of a Förster-type energy transfer (FRET)[19] mechanism because the exchange-type SET is normally negligible when R is longer than 5−10 Å.[20] The fast rate of FRET between $Py(S_1)$ to ImT is ascribed to the completely overlapped fluorescence spectrum of $Py(S_1)$ and the ground state absorption spectrum of ImT (Figure 3). Although the large orientation factor is not expected for Py and ImT, the SET rate was fast enough to avoid the generation of $Py(T_1)$ during the 355-nm first laser irradiation.

Thus, the selective generation of long-lived $Py(T_1)$ was achieved by utilizing the different energy transfer mechanisms.

Two-Step TET Mechanism. In order to reveal the two-step TET mechanism via $Ph_2(T_1)$, the TET process was also investigated with $(Py\text{-}Ph)_2$-ImT, in which Ph_2 of $(Py\text{-}Ph_2)_2$-ImT was changed to Ph with higher T_1 energy than Ph_2. If the TET from $ImT(T_n)$ to Py occurs directly, the TET from $ImT(T_n)$ should be observed even after changing Ph_2 to Ph. As a result, no bleaching of the absorption of $ImT(T_1)$ was observed for $(Py\text{-}Ph)_2$-ImT during the ns−ns 2-LFP (Figure S4), indicating that $Ph(T_1)$ is not accessible from $ImT(T_n)$ because of the higher E_{T1} of Ph than that of Ph_2. Therefore, this result indicates that the TET from $ImT(T_n)$ to Py takes place via $Ph_2(T_1)$.

Intramolecular TET in $(Py\text{-}Ph_2)_2$-ImT during Nanosecond−Picosecond Two-Color Two-Laser Flash Photolysis. The intramolecular TET from $ImT(T_n)$ to Ph_2 occurs competitively with the IC from $ImT(T_n)$ to $ImT(T_1)$ (eq 4).

$$(Py\text{-}Ph_2)_2\text{-}ImT(T_n) \xrightarrow{TET} (Py\text{-}Ph_2(T_1))_2\text{-}ImT \quad (4)$$
$$(Py\text{-}Ph_2)_2\text{-}ImT(T_n) \xrightarrow{IC} (Py\text{-}Ph_2)_2\text{-}ImT(T_1)$$

Then, the TET from $Ph_2(T_1)$ to Py proceeds in competition with the back-TET from $Ph_2(T_1)$ to ImT (eq 5).

$$(Py\text{-}Ph_2(T_1))_2\text{-}ImT \xrightarrow{TET} (Py(T_1)\text{-}Ph_2)_2\text{-}ImT \quad (5)$$
$$(Py\text{-}Ph_2(T_1))_2\text{-}ImT \xrightarrow{Back\ TET} (Py\text{-}Ph_2)_2\text{-}ImT(T_1)$$

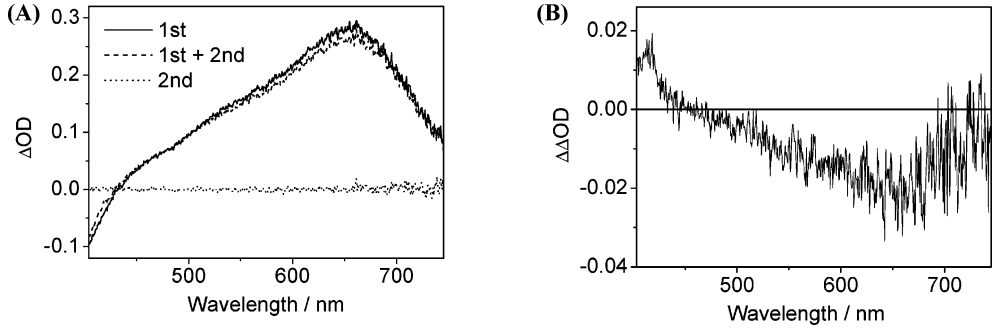

Figure 4. (A) Transient absorption spectra of $(Py\text{-}Ph_2)_2$-ImT in THF at 1.2 μs during the ns−ns 2-LFP (first laser, 355 nm, fwhm 5 ns, 5 mJ pulse^{-1}; second laser, 532 nm, 5-ns fwhm, 8 mJ pulse^{-1}). The second laser was irradiated at 1 μs after the first laser. The solid, dashed, and dotted lines show the 355-nm single-laser, two-laser, and 532-nm single-laser flash photolysis, respectively. (B) Difference spectrum of transient absorption spectra of $(Py\text{-}Ph_2)_2$-ImT during the 355-nm single-laser and two-laser flash photolysis.

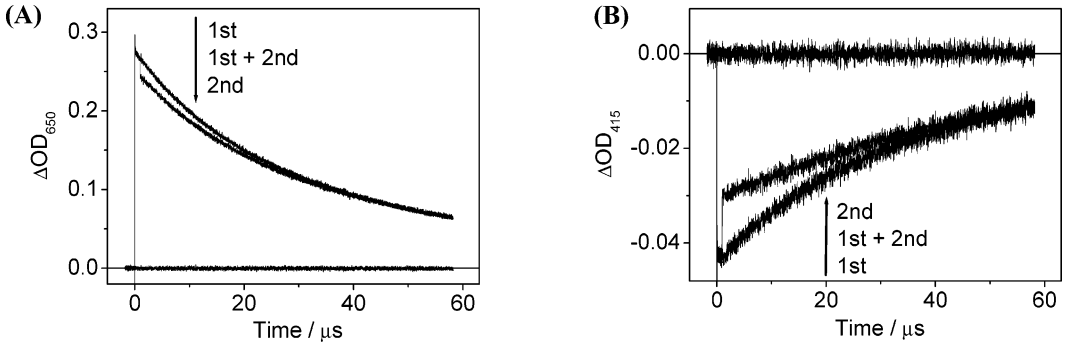

Figure 5. Time profiles of ΔOD at 650 nm (A) and 415 nm (B) of $(Py\text{-}Ph_2)_2$-ImT in THF during the ns−ns 2-LFP (first laser, 355 nm, 5-ns fwhm, 5 mJ pulse^{-1}; second laser, 532 nm, 5-ns fwhm, 8 mJ pulse^{-1}). The second laser was irradiated at 1 μs after the first laser.

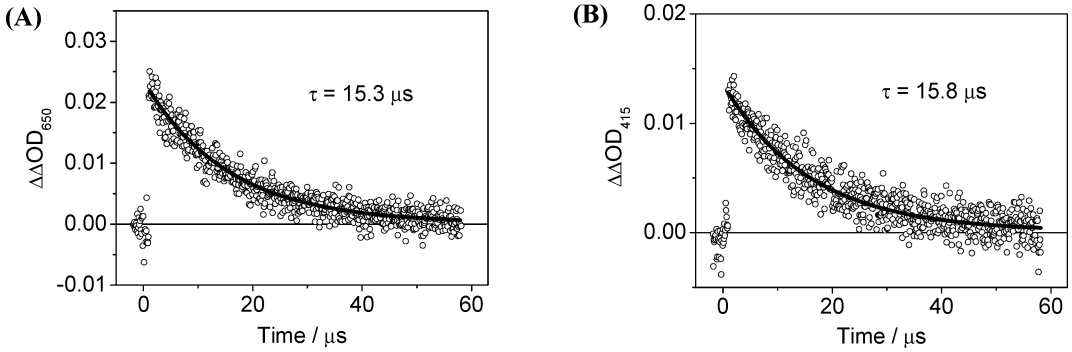

Figure 6. Time profiles of ΔΔOD at 650 nm [(355-nm single-laser) − (two-laser), (A)] and 415 nm [(two-laser) − (355-nm single-laser), (B)] of $(Py\text{-}Ph_2)_2$-ImT. The solid lines are the fitted lines.

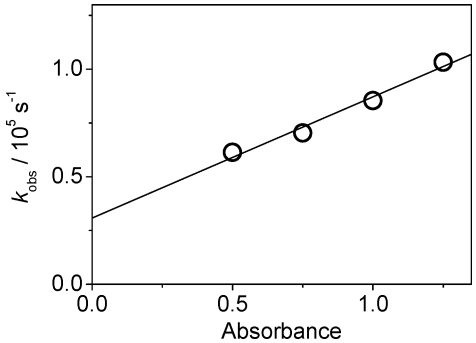

Figure 7. Plots of the triplet energy transfer rate from $Py(T_1)$ to ImT vs absorbance at 355 nm of $(Py\text{-}Ph_2)_2$-ImT. The solid line is the fitted line. The absorbance at 355 nm of $(Py\text{-}Ph_2)_2$-ImT was used instead of the concentration.

Recently, we have directly estimated the IC rates from the T_n to T_1 state to be a few tens of picoseconds for some aromatic compounds by using the ns−ps 2-LFP.[7] On the other hand, Hayes et al. have estimated the TET rates from perylene(T_n) to Zn−porphyrin and from Zn−porphyrin(T_1) to perylene to be 600 fs and 55 ns, respectively, when the dyads have a linkage at the imide-nitrogen.[6b] By assuming the similar TET and IC rates of the previous studies for $(Py\text{-}Ph_2)_2$-ImT, the TET from ImT(T_n) to Ph_2 is the predominant process in eq 4. In addition, the intramolecular TET rate from benzophenone(T_1) to naphthalene linked with a methylene spacer has been estimated to be 20 ps.[8] Therefore, the rates of the TET processes from ImT-(T_n) to Ph_2 and from $Ph_2(T_1)$ to Py will be significantly faster than the competing processes.

To confirm the fast and efficient TET processes from ImT(T_n) to Py, ns−ps 2-LFP was carried out. Figure 8A shows the time profiles of ΔOD at 650 nm during the ns−ps 2-LFP of *tert*-butylbiphenyl-substituted ImT [$(Ph_2)_2$-ImT, Figure 8A, inset]. Upon the second laser irradiation, the bleaching of the absorption of ImT(T_1) followed by recovery process was observed. The recovery was fitted by a single-exponential function and the rate was estimated to be 4.4×10^9 s^{-1}, corresponding to the lifetime of 230 ps. The recovery process

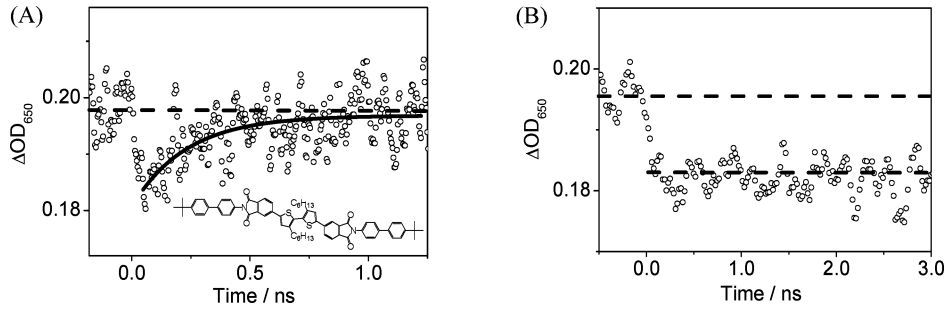

Figure 8. Time profiles of ΔOD at 650 nm of $(Ph_2)_2$-ImT (A) and $(Py\text{-}Ph_2)_2$-ImT (B) in THF during the ns−ps 2-LFP (first laser, 355 nm, fwhm 5 ns, 13 mJ pulse^{-1}; second laser, 532 nm, 30-ps fwhm, 30 mJ pulse^{-1}). The second laser was irradiated at 1 μs after the first laser. The solid line is the fitted line. Inset: molecular structure of $(Ph_2)_2$-ImT.

can be assigned to the TET from $Ph_2(T_1)$ to ImT, because the lifetime of $(CH)_2$-ImT(T_n) was estimated to be a few tens of picoseconds (data not shown) as well as some other aromatic compounds.[7] The back-TET rate from $Ph_2(T_1)$ to ImT is significantly faster than that from Zn−porphyrin(T_1) to perylene. However, for $(Py\text{-}Ph_2)_2$-ImT, only bleaching of the absorption of ImT(T_1) was observed without a recovery process during the ns−ps 2-LFP (Figure 8B), indicating the TET from $Ph_2(T_1)$ to Py is the predominant process.

Although it is difficult to estimate directly the TET rate from ImT(T_n) to Ph_2 due to the time resolution limit of our apparatus, it is expected that the TET from ImT(T_n) to Ph_2 is efficient. Because the recovery of ImT(T_1) absorption in Figure 8A can be fitted by a single-exponential function, if the TET from ImT(T_n) to Ph_2 is inefficient, the fast component due to the internal conversion process from ImT(T_n) to ImT(T_1) should be observed in the recovery process.

Hence, the two-step TET from ImT(T_n) to Py through Ph_2 during the 2-LFP is considered to be an efficient process.

Conclusions

In summary, we elucidated the energy transfer processes in $(Py\text{-}Ph_2)_2$-ImT during the 2-LFP. The singlet excitation energy was harvested into the center ImT, and then, ImT(T_1) was predominantly generated via intersystem crossing. ImT(T_n) generated with the second 532-nm laser irradiation caused intramolecular TET to Py via a two-step TET through Ph_2, resulting in selective generation of long-lived Py(T_1) efficiently. Furthermore, the triplet energy flow can be controlled in a molecular array such as $(-X-N-Y-CH_2-)_n$, in which chromophore Y has a lower E_{T1} than that of chromophore X, and $-N-$ and $-CH_2-$ are an imide bond and a methylene spacer, respectively. The triplet energy flow from Y(T_n) is defined to be from the imide (left) side and the TET processes are repeatable. Therefore, this behavior can be used as an efficient molecular size shift register.[6a]

Experimental Section

Materials. $(Py\text{-}Ph_2)_2$-ImT was synthesized according to Scheme 2. Biarylmethanol was synthesized by Grignard coupling, and then, the hydroxy group was reduced using Me_2-SiHCl/$InCl_3$ system.[21] The aminobiphenyl unit was produced by Suzuki-cross coupling. 4-Bromophthalic anhydrous was attached with the amino group by refluxing in toluene/DMF in the presence of triethylamine. 3,3′-Dihexyl-5,5′-bis(tributylstannanyl)-[2,2′]bithiophenyl was prepared according to the literature.[22] Finally, $(Py\text{-}Ph_2)_2$-ImT was produced by Pd-catalyzed Stille cross-coupling. Other reagents and solvents were commercially available.

General Information. Gel permeation chromatograph (GPC) was performed on a Japan Analytical Industry Co. Ltd. LC908 recycling preparative high-performance liquid chromatograph. The ^{1}H NMR spectra of the samples were recorded using a JEOL JMN EX-270 (270 MHz). The MS spectrometry was performed using JEOL JMS-600H FAB and Shimazu AXIMA-LNR MALDI-TOF spectrometers, utilizing 3-nitrobenzyl alcohol and 3-hydroxypicolinic acid, respectively.

(4-Bromophenyl)pyren-1-ylmethanol (1). 4-Bromobenzaldehyde was added dropwise to a solution of (pyrene-1-yl)-magnesium bromide prepared from 1-bromopyrene (1.0 g, 3.6 mmol), magnesium (0.090 g, 3.74 mmol), and a catalytic amount of iodine in THF (10 mL). The reaction mixture was stirred for 3 h at room temperature and then quenched by the addition of an aqueous solution of NH_4Cl. The organic layer was extracted with ether and washed with water and brine. The solution was dried over Na_2SO_4. The solvent was removed in vacuo. The residue was purified by silica column (eluent, 3:1 *n*-hexane−dichloromethane) to give a yellow solid (1.05 g, 76%). ^{1}H NMR (270 MHz, $CDCl_3$): δ 2.51 (d, J = 3.8 Hz, 1H), 6.82 (d, J = 3.5 Hz, 1H), 7.32 (d, J = 8.6 Hz, 2H), 7.45 (d, J = 8.6 Hz, 2H), 7.98−8.31 (m, 9H). FAB-MS (MW = 387.28): m/z = 385.2.

1-(4-Bromobenzyl)pyrene (2). To a solution of **1** (1.0 g, 2.6 mmol) and $InCl_3$ (0.029 g, 0.13 mmol) in 30 mL of CH_2Cl_2 was added Me_2SiHCl (0.69 mL, 6.2 mmol). The solution was stirred for 6 h at room temperature. The reaction mixture was diluted with CH_2Cl_2 and washed with water and brine. After being dried over Na_2SO_4, the solvent was removed in vacuo. The residue was purified by a silica column (eluent, 10:1 *n*-hexane−dichloromethane) to give the white solid (0.82 g, 86%). ^{1}H NMR (270 MHz, $CDCl_3$): δ 4.68 (s, 2H), 7.06 (d, J = 8.6 Hz, 2H), 7.36 (d, J = 8.4 Hz, 2H), 7.84−8.19 (m, 9H). FAB-MS (MW = 371.28): m/z = 371.9.

4′-Pyren-1-ylmethylbiphenyl-4-ylamine (3). A solution of **2** (1.42 g, 3.8 mmol), 4-aminophenylboronic acid, pinacol ester (1.0 g, 4.6 mmol), and tetrakis(triphenylphosphine)palladium (0.22 g, 0.19 mmol) in toluene (45 mL) was stirred under Ar atmosphere at room temperature for 30 min. Then, an aqueous solution of Na_2CO_3 (2 M, 10 mL) was added. The resulting mixture was heated under reflux for 12 h. The cooled mixture was extracted with toluene and washed with water and brine. The solution was dried over Na_2SO_4 and the solvent was removed in vacuo. The residue was purified by silica column (eluent, 2:1 *n*-hexane−ethyl acetate) to give a white solid (1.15 g, 78%). ^{1}H NMR (270 MHz, $CDCl_3$): δ 3.67 (s, 2H), 4.76 (s, 2H), 6.71 (d, J = 8.4 Hz, 2H), 7.22 (d, J = 7.8 Hz, 2H), 7.36 (d, J = 8.4 Hz, 2H), 7.89−8.30 (m, 9H). FAB-MS (MW = 383.5): m/z = 384.1.

SCHEME 2: Synthetic Route of (Py-Ph$_2$)$_2$-ImT

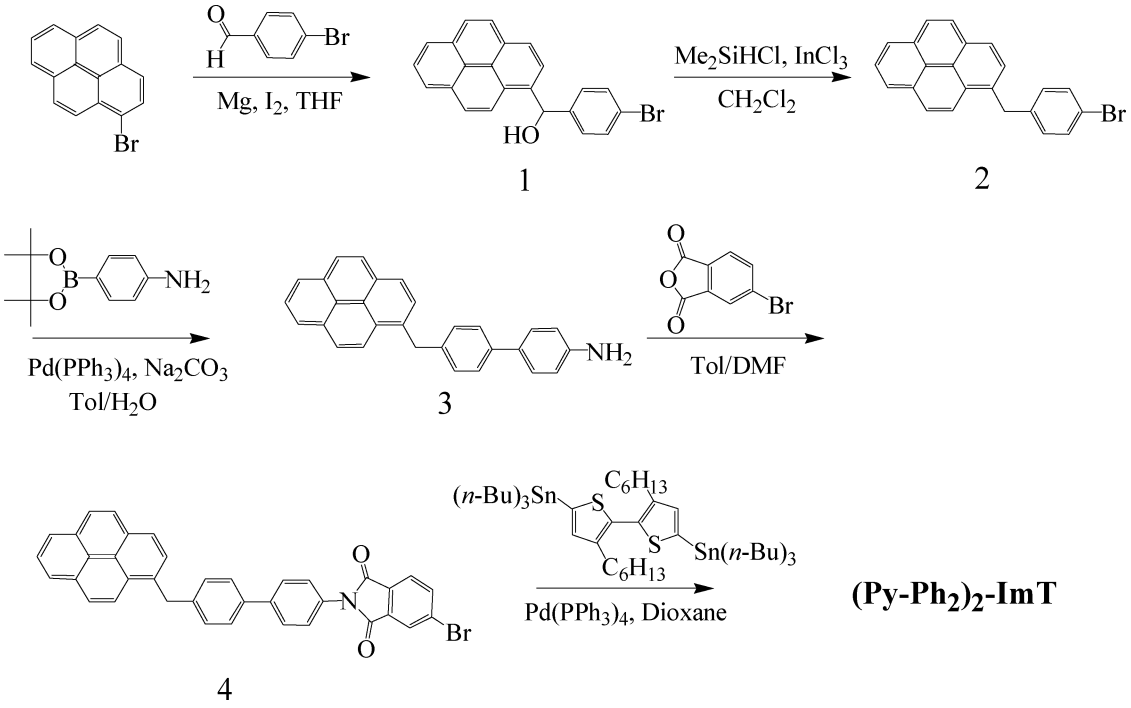

5-Bromo-2-(4′-pyren-1-ylmethylbiphenyl-4-yl)isoindole-1,3-dione (4). A solution of **3** (1.42 g, 3.8 mmol), 4-bromophthalic anhydrous (0.82 g, 3.6 mmol), and triethylamine (0.1 mL) in toluene (38 mL) and DMF (7.7 mL) was refluxed for 12 h. To the solution was added ethanol (100 mL), and the precipitate was collected by filtration. The solids were washed with acetone several times, dissolved in CH_2Cl_2, and washed with water and brine. The solution was dried over Na_2SO_4. The solvent was removed in vacuo. **4** was obtained as a slightly yellow solid (1.36 g, 77%). ^{1}H NMR (270 MHz, $CDCl_3$): δ 4.80 (s, 2H), 7.30 (d, 8.4 Hz 2H), 7.46 (d, J = 8.6 Hz, 2H), 7.50 (d, J = 8.1 Hz, 2H), 7.66 (d, J = 8.6 Hz, 2H), 7.81 (d, J = 8.1 Hz), 7.90−8.20 (m, 10H), 8.28 (d, J = 9.5 Hz, 1H). FAB-MS (MW = 592.5): m/z = 592.8.

(Py-Ph$_2$)$_2$-ImT. The solution of **4** (0.43 g, 0.73 mmol) and 3,3′-dihexyl-5,5′-bis(tributylstannanyl)[2,2′]bithiophenyl (0.30 g, 0.33 mmol) in dioxane (15 mL) was stirred for 30 min under Ar atmosphere at room temperature, followed by addition of tetrakis(triphenylphosphine)palladium (0.042 g, 0.036 mmol). The reaction mixture was stirred for 30 h at 100 °C. The solution was treated with boiling chloroform. After cooling, the precipitates were corrected by filtration. The sample was purified by a silica column (eluent, 10:1 chloroform−acetone) to give an orange solid (0.27 g, 61%). ^{1}H NMR (270 MHz, $CDCl_3$): δ 0.86 (t, J = 5.1 Hz, 6H), 1.28−1.32 (m, 12H), 1.51−1.72 (m, 4H), 2.62 (t, J = 7.6 Hz, 4H), 4.79 (s, 4H), 7.30 (d, J = 8.6 Hz, 4H), 7.42 (s, 2H), 7.50 (d, J = 8.9 Hz, 4H), 7.51 (d, J = 8.9 Hz, 4H), 7.90−8.17 (m, 22H), 8.29 (d, J = 9.2 Hz, 2H). MALDI-TOF MS (MW = 1357.76): m/z = 1357.6.

Phosphoric Acid Diethyl Ester Pyren-1-ylmethyl Ester. To a solution of 1-pyrenemethanol (0.20 g, 0.86 mmol), triethylamine (0.13 g, 1.29 mmol), and dimethylaminopyridine (0.011 g, 0.086 mmol) in THF (1 mL) was slowly added diethylchlorophosphate (0.13 mL). The reaction mixture was stirred for 4 h at room temperature before it was poured into a mixture of 2 M $KHSO_4$ (1 mL) and water (10 mL). The desired product was extracted by ether and washed with saturated aqueous $NaHCO_3$ and brine. The organic layer was dried over Na_2SO_4 and then the solvent was evaporated in vacuo. The crude oil was purified by a silica column (eluent, 1:2 *n*-hexane−ethyl acetate) to give a yellow oil (0.29 g, 91%). ^{1}H NMR (270 MHz, $CDCl_3$): δ 1.25 (t, J = 6.8 Hz, 6H), 4.00−4.12 (m, 4H), 5.81 (d, J = 8.1 Hz, 2H), 8.00−8.25 (m, 8H), 8.39 (d, J = 9.5 Hz, 1H). FAB-MS (MW = 368.37): m/z = 368.4.

4-Pyren-1-ylmethylphenylamine. Palladium acetate (3.1 mg, 0.014 mmol) and triphenylphosphine (0.015 g, 0.057 mmol) were dissolved in toluene (2.0 mL) and transferred into a flask containing phosphoric acid diethyl ester pyren-1-ylmethyl ester (0.28 g, 0.76 mmol), 4-aminophenylboronic acid, pinacol ester (0.20 g, 0.91 mmol), and K_2CO_3 (0.10 g, 0.72 mmol) in toluene (3.0 mL). The vigorously stirred mixture was heated to 90 °C for 16 h under Ar. The reaction solution was subjected to aqueous workup using water and then brine, with dichloromethane as the extraction solvent, and dried over Na_2SO_4. After the solvent was removed in vacuo, the crude products were purified by a silica column (eluent, dichloromethane) to give the yellow solid (0.15 g, 64%). ^{1}H NMR (270 MHz, $CDCl_3$): δ 3.55 (s, 2H), 4.64 (s, 2H), 6.60 (d, J = 8.2 Hz, 2H), 7.00 (d, J = 8.2 Hz, 2H), 7.86 (d, J = 7.9 Hz, 1H), 7.98 (t, J = 7.8 Hz, 1H), 8.03−8.17 (m, 6H), 8.27 (d, J = 9.4 Hz, 1H). FAB-MS (MW = 307.4): m/z = 307.4.

5-Bromo-2-(4-pyren-1-ylmethylphenyl)isoindole-1,3-dione. A solution of 4-pyren-1-ylmethylphenylamine (0.15 g, 0.49 mmol), 4-bromophthalic anhydride (0.13 g, 0.57 mmol), and triethylamine (0.1 mL) in toluene (6 mL) and DMF (1 mL) was refluxed for 12 h. The reaction solution was subjected to aqueous workup using water and then brine, with dichloromethane as the extraction solvent, and dried over Na_2SO_4. After the solvent was removed in vacuo, the crude products were purified by a silica column (eluent, dichloromethane) to give the yellow solid (0.18 g, 71%). ^{1}H NMR (270 MHz, $CDCl_3$): δ 4.80 (s, 2H), 7.30 (d, J = 8.9, 2H), 7.34 (d, J = 8.9 Hz, 2H), 7.79 (q, J = 0.47, 7.9 Hz, 1H), 7.89−7.92 (m, 2H), 8.00 (t, J = 7.7 Hz, 1H), 8.09 (d, J = 9.4 Hz, 1H), 8.16−8.20 (m, 3H), 8.24 (d, J = 9.2 Hz, 1H). FAB-MS (MW = 516.4): m/z = 515.4.

(Py-Ph)$_2$-ImT. A solution of 5-bromo-2-(4-pyren-1-ylmethylphenyl)isoindole-1,3-dione (0.10 g, 0.19 mmol) and 3,3′-dihexyl-5,5′-bis(tributylstannanyl)[2,2′]bithiophenyl (0.080 g,

0.087 mmol) in dioxane (4.0 mL) was stirred for 30 min under an Ar atmosphere at room temperature, followed by the addition of tetrakis(triphenylphosphine)palladium (0.011 g, 0.0095 mmol). The reaction mixture was stirred for 10 h at 100 °C. The sample was purified by a silica column (eluent, dichloromethane) and then HPLC (gel permeation chromatography, chloroform) to give an orange solid (0.053 g, 50%). ^{1}H NMR (270 MHz, $CDCl_3$): δ 0.85 (t, J = 6.8 Hz, 6H), 1.27 (m, 12H), 1.63 (m, 4H), 2.60 (t, J = 7.3 Hz, 4H), 4.81 (s, 4H), 7.35 (s, 8H), 7.42 (s, 2H), 7.90 (m, 6H), 8.00 (t, J = 7.7 Hz, 2H), 7.07 (d, J = 1.2 Hz, 4H), 8.10 (d, J = 9.4 Hz, 2H), 8.14−8.20 (m, 8H), 8.25 (d, J = 9.2 Hz, 2H). MALDI-TOF MS (MW = 1205.56): m/z = 1205.9.

5-Bromo-2-(4-iodophenyl)isoindole-1,3-dione. A solution of 4-iodoaniline (1.0 g, 4.6 mmol), 4-bromophthalic anhydrous (0.89 g, 5.0 mmol), and triethylamine (0.7 mL) in toluene (40 mL) and DMF (5 mL) was refluxed for 12 h. The reaction solution was subjected to aqueous workup using water and then brine, with dichloromethane as the extraction solvent, and dried over Na_2SO_4. After the solvent was removed in vacuo, the crude products were purified by silica column (eluent, 1:4 *n*-hexane−ethyl acetate) to give a yellow solid (0.18 g, 71%). ^{1}H NMR (270 MHz, $CDCl_3$): δ 7.19−7.23 (m, 2H), 7.79−7.86 (m, 3H), 7.94 (q, J = 1.6, 8.1 Hz, 1H), 8.09 (d, J = 0.54 Hz, 1H). FAB-MS (MW = 428.03): m/z = 427.3.

5-Bromo-2-(4′-*tert*-butylbiphenyl-4-yl)isoindole-1,3-dione. A solution of 5-bromo-2-(4-iodophenyl)isoindole-1,3-dione (0.76 g, 1.8 mmol), 4-*tert*-butylphenylbronic acid (0.35 g, 2.0 mmol), and tetrakis(triphenylphosphine)palladium (0.10 g, 0.087 mmol) in toluene (20 mL) was stirred under an Ar atmosphere at room temperature for 30 min. Then, an aqueous solution of Na_2CO_3 (2 M, 5 mL) was added. The resulting mixture was stirred for 12 h at 80 °C. The cooled mixture was extracted with toluene and washed with water and brine. The solution was dried over Na_2SO_4 and solvent was removed in vacuo. The residue was purified by a silica column (eluent, 2:1 *n*-hexane−ethyl acetate) to give the white solid (1.15 g, 78%). ^{1}H NMR (270 MHz, $CDCl_3$): δ 1.34 (s, 9H), 7.49 (d, J = 8.6 Hz, 4H), 7.56 (d, J = 8.6 Hz, 2H), 7.71 (d, J = 8.1 Hz, 2H), 7.84 (d, J = 7.8 Hz, 1H), 7.94 (d, J = 8.1 Hz, 1H), 8.11 (s, 1H). FAB-MS (MW = 434.34): m/z = 433.7.

$(Ph_2)_2$-ImT. A solution of 5-bromo-2-(4′-*tert*-butylbiphenyl-4-yl)isoindole-1,3-dione (0.30 g, 0.69 mmol) and 3,3′-dihexyl-5,5′-bis(tributylstannanyl)[2,2′]bithiophenyl (0.25 g, 0.27 mmol) in dioxane (12 mL) was stirred for 30 min under an Ar atmosphere at room temperature, followed by the addition of tetrakis(triphenylphosphine)palladium (0.040 g, 0.035 mmol). The reaction mixture was stirred for 30 h at 100 °C. The solution was treated with boiling chloroform. After cooling, the precipitates were corrected by filtration. The sample was purified by a silica column (eluent, 1:1 *n*-hexane−dichloromethane) to give the orange solid (0.10 g, 35%). ^{1}H NMR (270 MHz, $CDCl_3$): δ 0.87 (t, J = 6.5 Hz, 6H), 1.23−1.35 (m, 12H), 1.38 (s, 9H), 1.55−1.72 (m, 4H), 2.63 (t, J = 7.6 Hz, 4H), 7.46−7.75 (m, 14H), 7.71−7.76 (m, 4H), 7.95−8.02 (m, 4H), 8.20 (d, J = 0.81 Hz, 2H). MALDI-TOF MS (MW = 1041.44): m/z = 1044.3.

$(CH)_2$-ImT. A solution of 5-bromo-2-cyclohexylisoindoline-1,3-dione[23] (0.5 g, 1.62 mmol) and 3,3′-dihexyl-5,5′-bis(tributylstannanyl)[2,2′]bithiophenyl (0.59 g, 0.65 mmol) in DMF (5 mL) was stirred for 30 min under an Ar atmosphere at room temperature, followed by the addition of tetrakis(triphenylphosphine)palladium (0.094 g, 0.081 mmol). The reaction mixture was stirred for 30 h at 100 °C. The solution was diluted with CH_2Cl_2 and washed with water and brine. After being dried over Na_2SO_4, the solvent was removed in vacuo. The sample was purified by silica column (eluent, 10:1 *n*-hexane−ethyl acetate) to give a yellow solid (0.10 g, 20%). ^{1}H NMR (270 MHz, $CDCl_3$): δ 0.86 (t, J = 6.2 Hz, 6H), 1.26−1.91 (m, 32H), 2.17 (m, 4H) 2.60 (t, J = 7.6 Hz, 4H), 4.12 (m, 2H), 7.39 (s, 2H), 7.80 (d, 2H), 7.87 (q, J = 1.6, 7.8 Hz, 2H), 8.02 (d, J = 1.6 Hz, 2H). FAB-MS (MW = 789.12): m/z = 790.

Molecular Orbital Calculation. The MO calculation was performed at the PM3 level with the MOPAC 6.0.

Apparatus. Steady-state absorption and fluorescence spectra were measured on a Shimadzu UV-3100PC and a Hitachi 850, respectively.

The time-resolved fluorescence measurements in the picosecond to nanosecond time region were carried out by the single-photon counting method.[24] For excitation of the sample, the output of the Ti:sapphire laser (Spectra-Physics, Tsunami 3941-M1BB, fwhm 100 fs) was converted to THG (300 nm) with a harmonic generator (Spectra-Physics, GWU-23FL). Fluorescence from the sample was detected using a streak camera [Hamamatsu Photonics (4354)] equipped with a polychromator (Acton Research Spectra Pro 150).

The nanosecond−nanosecond two-color two-laser flash photolysis experiment was performed using the third harmonic oscillation (355 nm) of a Nd^{3+}:YAG laser (Quantel, Brilliant; 5 ns fwhm) as the first laser and the second harmonic oscillation (532 nm) of a Nd^{3+}:YAG laser (Continuum, Surelite II-10; 5 ns fwhm) as the second laser. The delay time of two laser flashes was adjusted to 1 μs by three four-channel digital delay/pulse generators. Two laser beams were adjusted to overlap at the sample. The monitor light source was a 450 W xenon lamp (Osram, Model XBO-450) that was synchronized with the laser flash. The monitor light perpendicular to the laser beams was focused on a monochromator (Nikon, Model G250). The output of the monochromator was monitored using a photomultiplier tube (PMT) (Hamamatsu Photonics, Model R928). The signal from the PMT was recorded on a transient digitizer (Tektronix, Model TDS 580D four-channel digital phosphor oscilloscope). A multichannel analyzer system (Hamamatsu Photonics, C5967) was used for the measurement of the transient absorption spectra. The total system was controlled with a personal computer via a GP-IB interface.

The nanosecond−picosecond two-color two-laser flash photolysis experiment was performed using the third harmonic oscillation (355 nm) of a nanosecond Nd^{3+}:YAG laser [Quantel, Brilliant; 5 ns full width at half-maximum (fwhm)] as the first laser and the second harmonic oscillation (532 nm) of a picosecond Nd^{3+}:YAG laser (Continuum, RGA69−10; 30 ps fwhm) as the second laser. The delay time of the two laser flashes was adjusted to 1 μs by four-channel digital delay/pulse generators (Stanford Research Systems, Model DG 535). The breakdown of xenon gas generated by the fundamental pulse of the picosecond Nd^{3+}:YAG laser was used as a probe light. Transient absorption spectra and kinetic traces were measured using a streak camera (Hamamatsu Photonics, Model C7700) that was equipped with a charge-coupled device (CCD) camera (Hamamatsu Photonics, Model C4742-98) and were stored on a personal computer (PC). In the case of the nanosecond−picosecond two-color two-laser flash photolysis of $(CH)_2$-ImT, the lifetime of $(CH)_2$-ImT(T_n) is close to the time resolution limit of our apparatus (30 ps). Therefore, it was difficult to properly estimate the internal conversion rate from $(CH)_2$-ImT-(T_n) to $(CH)_2$-ImT(T_1).

Acknowledgment. This work has been partly supported by a Grant-in-Aid for Scientific Research (Project 17105005, 19350069, and others) from the Ministry of Education, Culture, Sports, Science and Technology (MEXT) of the Japanese Government.

Supporting Information Available: The synthesis of $(Py\text{-}Ph_2)_2$-ImT, $(Py\text{-}Ph)_2$-ImT, and $(CH)_2$-ImT, the absorption and fluorescence spectra of $(CH)_2$-ImT, the transient absorption spectra of $(CH)_2$-ImT during the ns laser flash photolysis, the molecular orbital calculation of $(Py\text{-}Ph_2)_2$-ImT, and time profiles of ΔOD at 650 nm of $(Py\text{-}Ph)_2$-ImT in THF during the ns−ns 2-LFP. This material is available free of charge via the Internet at http://pubs.acs.org.

References and Notes

(1) (a) Hu, X.; Damjanović, A.; Ritz, T.; Schulten, K. *Proc. Natl. Acad. Sci. U.S.A.* **1998**, *95*, 5935. (b) van Oijen, A. M.; Ketelaars, M.; Köhler, J.; Aartsma, T. J.; Schmidt, J. *Science* **1999**, *285*, 400.

(2) (a) Wasielewski, M. R. *Chem. Rev.* **1992**, *92*, 435. (b) Gust, D.; Moore, T. A.; Moore, A. L. *Acc. Chem. Res.* **2001**, *34*, 40. (c) Guldi, D. M. *Chem. Soc. Rev.* **2002**, *31*, 22. (d) Choi, M.-S.; Yamazaki, T.; Yamazaki, I.; Aida, T. *Angew. Chem. Int. Ed.* **2004**, *43*, 150. (e) Kim, D.; Osuka, A. *Acc. Chem. Res.* **2004**, *37*, 735. (f) Imahori, H. *Org. Biomol. Chem.* **2004**, *2*, 1425. (g) De Schryver, F. C.; Vosch, T.; Cotlet, M.; Van Der Auweraer, M.; Müllen, K.; Hofkens, J. *Acc. Chem. Res.* **2005**, *38*, 514.

(3) (a) Lukas, A. S.; Wasielewski, M. R. In *Electron Transfer in Chemistry*; Balzani, V., Ed.; Wiley-NCH: New York, 2001; Vol. 5, pp 48−96. (b) Andersson, M.; Sinks, L. E.; Hayes, R. T.; Zhao, Y.; Wasielewski, M. R. *Angew. Chem. Int. Ed.* **2003**, *42*, 3139. (c) Qu, D.-H.; Wang, Q.-C.; Tian, H. *Angew. Chem. Int. Ed.* **2005**, *44*, 5296. (d) Gust, D.; Moore, T. A.; Moore, A. L. *Chem. Commun.* **2006**, 1169. (e) de Silva, A. P.; Leydet, Y.; Lincheneau, C.; McClenaghan, N. D. *J. Phys. Condens. Matter* **2006**, *18*, 1847. (f) Andréasson, J.; Straight, S. D.; Kodis, G.; Park, C.-D.; Hambourger, M.; Gervaldo, M.; Albinsson, B.; Moore, T. A.; Moore, A. L.; Gust, D. *J. Am. Chem. Soc.* **2006**, *128*, 16259.

(4) (a) Turro, N. J.; Ramamurthy, V.; Cherry, W.; Rarneth, W. *Chem. Rev.* **1978**, *78*, 125. (b) McGimpsey, W. G. *Trends Org. Chem.* **1997**, *6*, 233. (c) Liu, R. S. H.; Edman, J. R. *J. Am. Chem. Soc.* **1968**, *90*, 213. (d) Ladwig, C. C.; Liu, R. S. H. *J. Am. Chem. Soc.* **1974**, *96*, 6210. (e) Ladwig, C. C.; Liu, R. S. H. *Chem. Phys. Lett.* **1975**, *35*, 563. (f) Ladwig, C. C.; Liu, R. S. H. *J. Am. Chem. Soc.* **1976**, *98*, 8093. (g) Koshihara, S.; Kobayashi, T. *J. Chem. Phys.* **1986**, *85*, 1211. (h) McGimpsey, W. G.; Scaiano, J. C. *J. Am. Chem. Soc.* **1988**, *110*, 2299. (i) McGimpsey, W. G.; Scaiano, J. C. *J. Am. Chem. Soc.* **1989**, *111*, 335. (j) McGimpsey, W. G.; Evans, C.; Bohne, C.; Kennedy, S. R.; Scaiano, J. C. *Chem. Phys. Lett.* **1989**, *161*, 342. (k) Bohne, C.; Kennedy, S. R.; Boch, R.; Negri, F.; Orlandi, G.; Siebrand, W.; Scaiano, J. C. *J. Phys. Chem.* **1991**, *95*, 10300. (l) Gannon, T.; McGimpsey, W. G. *J. Org. Chem.* **1993**, *58*, 5639.

(5) (a) Cai, X.; Hara, M.; Kawai, K.; Tojo, S.; Majima, T. *Chem. Commun.* **2003**, 222. (b) Cai, X.; Sakamoto, M.; Hara, M.; Tojo, S.; Fujitsuka, M.; Ouchi, A.; Majima, T. *Chem. Commun.* **2003**, 2604. (c) Cai, X.; Sakamoto, M.; Hara, M.; Fujitsuka, M.; Majima, T. *J. Am. Chem. Soc.* **2004**, *126*, 7432. (d) Sakamoto, M.; Cai, X.; Hara, M.; Fujitsuka, M.; Majima, T. *J. Am. Chem. Soc.* **2004**, *126*, 9709. (f) Cai, X.; Sakamoto, M.; Yamaji, M.; Fujitsuka, M.; Majima, T. *Chem.-Eur. J.* **2007**, *13*, 3143. (g) Oseki, Y.; Fujitsuka, M.; Sakamoto, M.; Cai, X.; Majima, M. *J. Phys. Chem. C* **2007**, *111*, 1024.

(6) (a) McGimpsey, W. G.; Samaniego, W. N.; Chen, L.; Wang, F. *J. Phys. Chem. A* **1998**, *102*, 8679. (b) Hayes, R. T.; Walsh, C. J.; Wasielewski, M. R. *J. Phys. Chem. A* **2004**, *108*, 3253. (c) Ren, Y.; Wang, Z.; Zhu, H.; Weininger, S. J.; McGimpsery, W. G. *J. Am. Chem. Soc.* **1995**, *117*, 4367.

(7) (a) Fujitsuka, M.; Oseki, Y.; Hara, M.; Cai, X.; Sugimoto, A.; Majima, T. *Chem. Phys. Chem.* **2004**, *5*, 1240. (b) Cai, X.; Sakamoto, M.; Hara, M.; Fujitsuka, M.; Majima, T. *J. Phys. Chem. A* **2004**, *108*, 7147. (c) Oseki, Y.; Fujitsuka, M.; Hara, M.; Cai, X.; Sugimoto, A.; Majima, T. *J. Phys. Chem. B* **2004**, *108*, 16727. (d) Cai, X.; Sakamoto, M.; Fujitsuka, M.; Majima, T. *Chem.-Eur. J.* **2005**, *11*, 6471.

(8) Closs, G. L.; Piotrowiak, P.; Maclnnis, J. M.; Fleming, G. R. *J. Am. Chem. Soc.* **1988**, *110*, 2652.

(9) (a) Tomizaki, K.; Loewe, R. S.; Kirmaier, C.; Schwartz, J. K.; Retsek, J. L.; Bocian, D. F.; Holten, D.; Lindsey, J. S. *J. Org. Chem.* **2002**, *67*, 6519. (b) Pasaogullari, N.; Icil, H.; Demuth, M. *Dyes Pigm.* **2006**, *69*, 118.

(10) (a) Samanta, A.; Ramachandram, B.; Saroja, G. *J. Photochem. Photobiol.* **1996**, *101*, 29. (b) Wintgens, V.; Valat, P.; Kossanyl, J.; Biczok, L.; Demeter, A.; Bérces, T. *J. Chem. Soc. Faraday Trans.* **1994**, *90*, 411.

(11) Cho, D. W.; Fujitsuka, M.; Sugimoto, A.; Yoon, U. C.; Mariano, P. S.; Majima, T. *J. Phys. Chem. B* **2006**, *110*, 11062.

(12) (a) Demeter, A.; Bérces, T.; Blczók, L.; Wintgens, V.; Valat, P.; Kossanyi. J. *J. Chem. Soc. Faraday Trans.* **1994**, *90*, 2635. (b) Wintgens, V.; Valat, P.; Kossanyi, J.; Demeter, A.; Biczók, L.; Bérces, T. *J. Chem. Soc. Faraday Trans.* **1996**, *93*, 109.

(13) (a) Matsumoto, K.; Fujitsuka, M.; Sato, T.; Onodera, S.; Onodera, S.; Ito, O. *J. Phys. Chem. B* **2000**, *104*, 11632. (b) Oseki, Y.; Fujitsuka, M.; Cho, D. W.; Sugimoto, A.; Tojo, S.; Majima, T. *J. Phys. Chem. B* **2005**, *109*, 19257. (c) Beek, W. J. E.; Janssen, R. A. J. *J. Mater. Chem.* **2004**, *14*, 2795.

(14) (a) Becker, R. S.; de Melo, J. S.; Macanita, A. L.; Elisei, F. *J. Phys. Chem.* **1996**, *100*, 18683. (b) Oseki, Y.; Fujitsuka, M.; Michihiro, H.; Cai, X.; Ie, Y.; Aso, Y.; Majima, T. *J. Phys. Chem. B* **2005**, *109*, 10695. (c) Pina, J.; Burrows, H. D.; Becker, R. S.; Dias, F. B.; Macanita, A. L.; Seixas de Melo, J. *J. Phys. Chem. B* **2006**, *110*, 6499.

(15) Murov, S. L. *Handbook of Photochemistry*, 2nd ed.; Marcel Dekker: New York, 1993.

(16) (a) Klán, P.; Wagner, P. J. *J. Am. Chem. Soc.* **1998**, *120*, 2198. Eng, M. P.; Ljungdahl, T.; Mårtensson, J.; Albinsson, Bo. *J. Phys. Chem. B* **2006**, *110*, 6483. (b) Eng, M. P.; Albinsson, B. *Angew. Chem. Int. Ed.* **2006**, *45*, 5626.

(17) Andéasson, J.; Kajanus, J.; Mårtensson, J.; Albinsson, B. *J. Am. Chem. Soc.* **2000**, *122*, 9844.

(18) Dexter, D. L. *J. Chem. Phys.* **1953**, *21*, 836.

(19) (a) Förster, T. *Naturwissenschaften* **1946**, *33*, 166. (b) Förster, T. *T. Ann. Phys.* **1948**, *2*, 55.

(20) Turro, N. J. *Modern Molecular Photochemistry*; University Science Books: Sausalito, CA, 1991.

(21) Miyai, T.; Ueba, M.; Baba, A. *Synlett* **1999**, *2*, 182.

(22) Nakazaki, J.; Chung, I.; Watanabe, R.; Ishitsuka, T.; Kawada, Y.; Matsushita, M. M.; Sugawara, T. *Internet Electron. J. Mol. Des.* **2003**, *2*, 112.

(23) Dautel, O. J.; Wantz, G.; Flot, D.; Lere-Porte, J.-P.; Moreau, J. J. E.; Parneix, J.-P.; Serein-Spirau, F.; Vignau, L. *J. Mat. Chem.* **2005**, *15*, 4446.

(24) Fujitsuka, M.; Okada, A.; Tojo, S.; Takei, F.; Onitsuka, K.; Takahashi, S.; Majima, T. *J. Phys. Chem. B* **2004**, *108*, 11935.